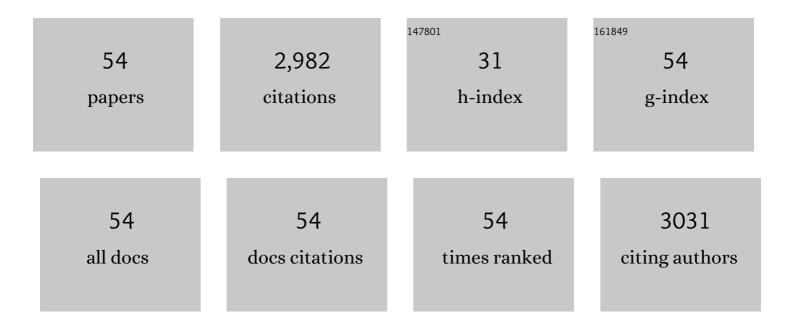
Qiming Xian

List of Publications by Year in descending order

Source: https://exaly.com/author-pdf/5729374/publications.pdf Version: 2024-02-01



#	Article	IF	CITATIONS
1	Ultrathin ZnIn ₂ S ₄ Nanosheets Anchored on Ti ₃ C ₂ T _{<i>X</i>} MXene for Photocatalytic H ₂ Evolution. Angewandte Chemie - International Edition, 2020, 59, 11287-11292.	13.8	416
2	0D/2D Co3O4/TiO2 Z-Scheme heterojunction for boosted photocatalytic degradation and mechanism investigation. Applied Catalysis B: Environmental, 2020, 278, 119298.	20.2	256
3	CeO2 nanocrystal-modified layered MoS2/g-C3N4 as 0D/2D ternary composite for visible-light photocatalytic hydrogen evolution: Interfacial consecutive multi-step electron transfer and enhanced H2O reactant adsorption. Applied Catalysis B: Environmental, 2019, 259, 118072.	20.2	158
4	Sources and environmental behavior of dechlorane plus — A review. Environment International, 2011, 37, 1273-1284.	10.0	153
5	Direct Z-scheme TiO2–ZnIn2S4 nanoflowers for cocatalyst-free photocatalytic water splitting. Applied Catalysis B: Environmental, 2021, 291, 120126.	20.2	147
6	Removal of nutrients and veterinary antibiotics from swine wastewater by a constructed macrophyte floating bed system. Journal of Environmental Management, 2010, 91, 2657-2661.	7.8	109
7	Enhanced photocatalytic water oxidation by hierarchical 2D-Bi2MoO6@2D-MXene Schottky junction nanohybrid. Chemical Engineering Journal, 2021, 403, 126328.	12.7	94
8	Detection, formation and occurrence of 13 new polar phenolic chlorinated and brominated disinfection byproducts in drinking water. Water Research, 2017, 112, 129-136.	11.3	89
9	Occurrence and ecological risk assessment of disinfection byproducts from chlorination of wastewater effluents in East China. Water Research, 2019, 157, 247-257.	11.3	89
10	Occurrence and health risk assessment of halogenated disinfection byproducts in indoor swimming pool water. Science of the Total Environment, 2016, 543, 425-431.	8.0	78
11	Facile synthesis of graphene nano zero-valent iron composites and their efficient removal of trichloronitromethane from drinking water. Chemosphere, 2016, 146, 32-39.	8.2	77
12	Isolation and Identification of Antialgal Compounds from the Leaves of Vallisneria spiralis L. by Activity-Guided Fractionation (5 pp). Environmental Science and Pollution Research, 2006, 13, 233-237.	5.3	74
13	Transformation among Aromatic Iodinated Disinfection Byproducts in the Presence of Monochloramine: From Monoiodophenol to Triiodophenol and Diiodonitrophenol. Environmental Science & Technology, 2017, 51, 10562-10571.	10.0	72
14	Edge-Rich Bicrystalline 1T/2H-MoS ₂ Cocatalyst-Decorated {110} Terminated CeO ₂ Nanorods for Photocatalytic Hydrogen Evolution. ACS Applied Materials & Interfaces, 2021, 13, 35818-35827.	8.0	65
15	Sol–gel based metal-organic framework zeolite imidazolate framework-8 fibers for solid-phase microextraction of nitro polycyclic aromatic hydrocarbons and polycyclic aromatic hydrocarbons in water samples. Journal of Chromatography A, 2019, 1603, 92-101.	3.7	64
16	Graphite-like carbon nitride coupled with tiny Bi2S3 nanoparticles as 2D/0D heterojunction with enhanced photocatalytic activity. Applied Surface Science, 2018, 444, 75-86.	6.1	55
17	Formation and toxicity of halogenated disinfection byproducts resulting from linear alkylbenzene sulfonates. Chemosphere, 2016, 149, 70-75.	8.2	54
18	Allelopathic activity of volatile substance from submerged macrophytes on Microcystin aeruginosa. Acta Ecologica Sinica, 2006, 26, 3549-3554.	1.9	51

QIMING XIAN

#	Article	IF	CITATIONS
19	Sheet-on-sheet TiO2/Bi2MoO6 heterostructure for enhanced photocatalytic amoxicillin degradation. Journal of Hazardous Materials, 2022, 421, 126634.	12.4	50
20	Formation of iodinated trihalomethanes and haloacetic acids from aromatic iodinated disinfection byproducts during chloramination. Water Research, 2018, 147, 254-263.	11.3	48
21	A novel molecularly imprinted polymer-solid phase extraction method coupled with high performance liquid chromatography tandem mass spectrometry for the determination of nitrosamines in water and beverage samples. Food Chemistry, 2019, 292, 267-274.	8.2	47
22	Metagenomic insights into tetracycline effects on microbial community and antibiotic resistance of mouse gut. Ecotoxicology, 2015, 24, 2125-2132.	2.4	46
23	Simultaneous determination of iodinated haloacetic acids and aromatic iodinated disinfection byproducts in waters with a new SPE-HPLC-MS/MS method. Chemosphere, 2018, 198, 147-153.	8.2	46
24	Carbon Nitride-Modified Defective TiO _{2–<i>x</i>} @Carbon Spheres for Photocatalytic H ₂ Evolution and Pollutants Removal: Synergistic Effect and Mechanism Insight. Journal of Physical Chemistry C, 2018, 122, 20444-20458.	3.1	45
25	DBPs formation and genotoxicity during chlorination of pyrimidines and purines bases. Chemical Engineering Journal, 2017, 307, 884-890.	12.7	41
26	Ultrafine Bi ₃ TaO ₇ Nanodot-Decorated V, N Codoped TiO ₂ Nanoblocks for Visible-Light Photocatalytic Activity: Interfacial Effect and Mechanism Insight. ACS Applied Materials & Interfaces, 2019, 11, 13011-13021.	8.0	41
27	Formation and Decomposition of New Iodinated Halobenzoquinones during Chloramination in Drinking Water. Environmental Science & Technology, 2020, 54, 5237-5248.	10.0	37
28	Nitrated and parent PAHs in the surface water of Lake Taihu, China: Occurrence, distribution, source, and human health risk assessment. Journal of Environmental Sciences, 2021, 102, 159-169.	6.1	36
29	Selection and applicability of quenching agents for the analysis of polar iodinated disinfection byproducts. Chemosphere, 2016, 163, 359-365.	8.2	34
30	Green and efficient synthesis of Co-MOF-based/g-C3N4 composite catalysts to activate peroxymonosulfate for degradation of the antidepressant venlafaxine. Journal of Colloid and Interface Science, 2022, 610, 280-294.	9.4	34
31	Characterization, DBPs formation, and mutagenicity of soluble microbial products (SMPs) in wastewater under simulated stressful conditions. Chemical Engineering Journal, 2015, 279, 258-263.	12.7	33
32	Photocatalytic degradation mechanism of phenanthrene over visible light driven plasmonic Ag/Ag3PO4/g-C3N4 heterojunction nanocomposite. Chemosphere, 2022, 293, 133575.	8.2	33
33	Molecularly imprinted solid phase extraction coupled with gas chromatography-mass spectrometry for determination of N-Nitrosodiphenylamine in water samples. Chemosphere, 2018, 212, 872-880.	8.2	29
34	Trihalomethane yields from twelve aromatic halogenated disinfection byproducts during chlor(am)ination. Chemosphere, 2019, 228, 668-675.	8.2	24
35	Formation of haloacetic acids from different organic precursors in swimming pool water during chlorination. Chemosphere, 2020, 247, 125793.	8.2	23
36	Comparative toxicity of chloro- and bromo-nitromethanes in mice based on a metabolomic method. Chemosphere, 2017, 185, 20-28.	8.2	22

QIMING XIAN

#	Article	IF	CITATIONS
37	Variation of levels and distribution of N-nitrosamines in different seasons in drinking waters of East China. Environmental Science and Pollution Research, 2015, 22, 11792-11800.	5.3	20
38	Rapid and complete dehalogenation of halonitromethanes in simulated gastrointestinal tract and its influence on toxicity. Chemosphere, 2018, 211, 1147-1155.	8.2	20
39	A highly selective fluorescent and chromogenic probe for CNâ^ detection and its applications in bioimaging. Talanta, 2018, 190, 487-491.	5.5	19
40	Analysis of traceâ€level nitrated polycyclic aromatic hydrocarbons in water samples by solidâ€phase microextraction with gas chromatography and mass spectrometry. Journal of Separation Science, 2018, 41, 2681-2687.	2.5	16
41	Study on the Structure and Mutagenicity of a New Disinfection Byproduct in Chlorinated Drinking Water. Environmental Science & Technology, 2005, 39, 7499-7508.	10.0	15
42	Cold on-column injection coupled with gas chromatography/mass spectrometry for determining halonitromethanes in drinking water. Analytical Methods, 2016, 8, 362-370.	2.7	15
43	Formation and influence factors of halonitromethanes in chlorination of nitro-aromatic compounds. Chemosphere, 2021, 278, 130497.	8.2	15
44	Occurrence of dissolved black carbon in source water and disinfection byproducts formation during chlorination. Journal of Hazardous Materials, 2022, 435, 129054.	12.4	14
45	Evaluation of DBPs formation from SMPs exposed to chlorine, chloramine and ozone. Journal of Water and Health, 2017, 15, 185-195.	2.6	12
46	Levels and distribution of Dechloranes in sediments of Lake Taihu, China. Environmental Science and Pollution Research, 2015, 22, 6601-6609.	5.3	11
47	Formation potential of N-nitrosamines from soluble microbial products (SMPs) exposed to chlorine, chloramine and ozone. RSC Advances, 2015, 5, 83682-83688.	3.6	9
48	Detection method and toxicity study of a new disinfection by-product, 2,2,4-trichloro-5-methoxycyclopenta-4-ene-1,3-dione (TCMCD), in chlorinated drinking water. Water Research, 2010, 44, 974-980.	11.3	8
49	NDMA adsorption and degradation by a new-type of Ag-MONT material carrying nanoscale zero-valent iron. Chemosphere, 2021, 268, 129271.	8.2	8
50	Photodegradation of acenaphthylene over plasmonic Ag/Ag3PO4 nanopolyhedrons synthesized via in-situ reduction. Applied Surface Science, 2022, 572, 151421.	6.1	8
51	All-solid-state Z-scheme heterostructures of 1T/2H-MoS2 nanosheets coupled V-doped hierarchical TiO2 spheres for enhanced photocatalytic activity. Materials Today Energy, 2022, 23, 100901.	4.7	8
52	Occurrence and transformation of newly discovered 2-bromo-6-chloro-1,4-benzoquinone in chlorinated drinking water. Journal of Hazardous Materials, 2022, 436, 129189.	12.4	8
53	ZIF-8/h-BN coated solid-phase microextraction fiber via physical coating technology and sol-gel technology for the determination of nitro polycyclic aromatic hydrocarbons from water samples. Microchemical Journal, 2022, 179, 107471.	4.5	5
54	Solidâ€phase microextraction combined with gas chromatography/triple quadrupole tandem mass spectrometry for determination of nitrated polycyclic aromatic hydrocarbons in sediments. Journal of Separation Science, 2022, , .	2.5	1